Supporting Information

A Tumor-pH-Responsive Supramolecular Photosensitizer for Activatable Photodynamic Therapy with Minimal *In Vivo* Skin Phototoxicity

Xingshu Li[1,2], Bi-Yuan Zheng[1], Mei-Rong Ke[1], Yongfan Zhang[1], Jian-Dong Huang[1]*, and Juyoung Yoon[2]*

1. College of Chemistry, State Key Laboratory of Photocatalysis on Energy and Environment, Fujian Provincial Key Laboratory of Cancer Metastasis Chemoprevention and Chemotherapy, Fuzhou University, Fuzhou 350108, China
2. Department of Chemistry and Nano Science, Ewha Womans University, Seoul 120-750, Korea

*Corresponding author: jdhuang@fzu.edu.cn; jyoon@ewha.ac.kr

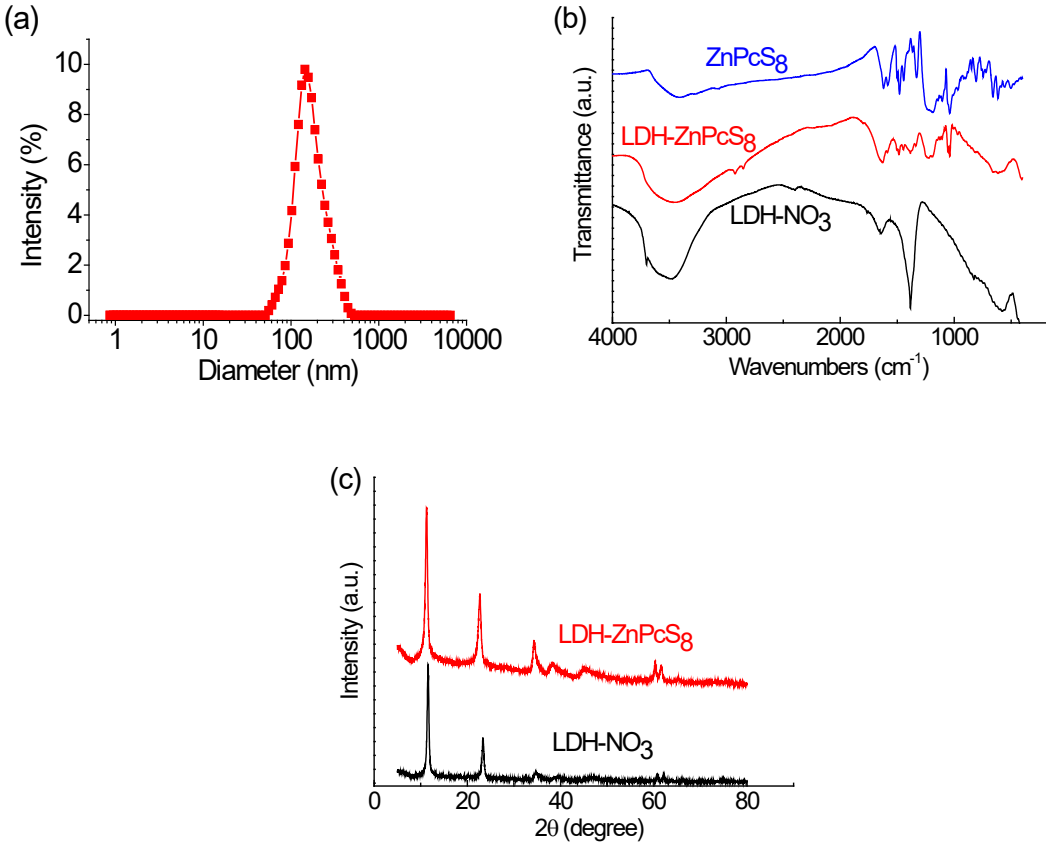

Figure S1. Characterization of LDH-$ZnPcS_8$. (a) DLS of LDH-$ZnPcS_8$. (b) FTIR spectra of $ZnPcS_8$, LDH-$ZnPcS_8$, and LDH-NO_3. (c) XRD patterns of LDH-$ZnPcS_8$ and LDH-NO_3.

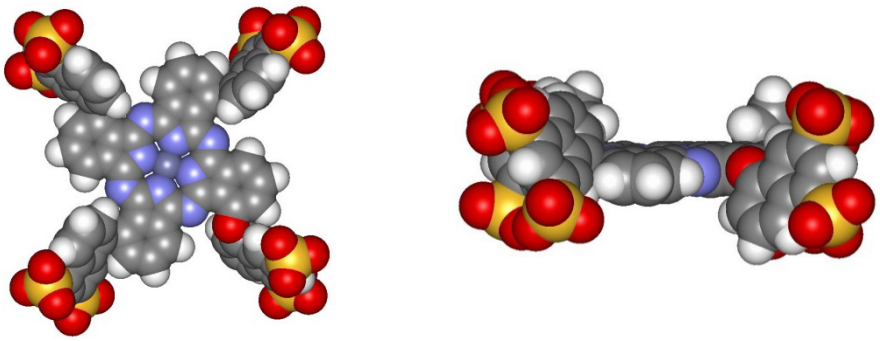

Top view Side view

Figure S2. Top view and side view of $ZnPcS_8$ structure. The three-dimension of $ZnPcS_8$ was calculated to be 2.00 × 2.00 × 0.85 nm by a PM3 method.

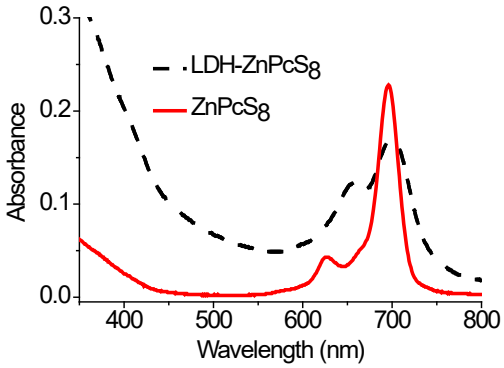

Figure S3. UV-vis spectra of $ZnPcS_8$ and LDH-$ZnPcS_8$ in water (both [$ZnPcS_8$] = 1.5 μM).

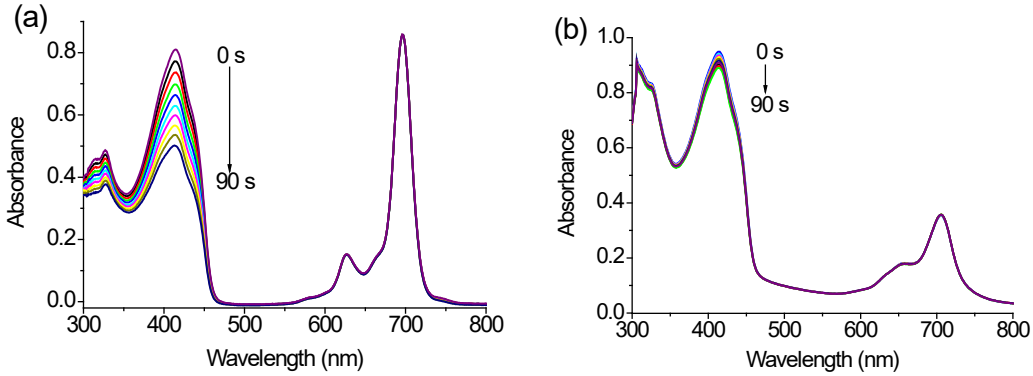

Figure S4. The UV-vis spectra of (a) $ZnPcS_8$ or (b) LDH-$ZnPcS_8$ (both [$ZnPcS_8$] = 3.5 μM) in the presence of DPBF (60 μM) in water (containing 0.12% DMF and 0.06% Cremophor EL) at different irradiation time.

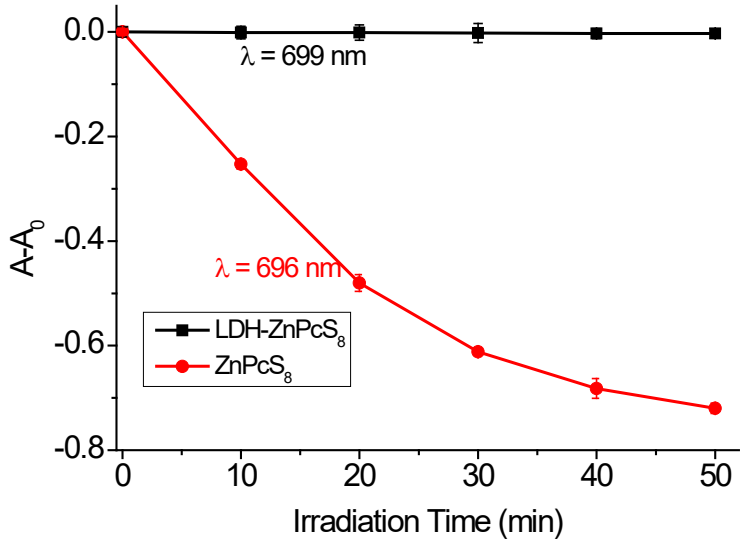

Figure S5. Comparison of the rates of photodegradation of $ZnPcS_8$ and LDH-$ZnPcS_8$ in water (both [$ZnPcS_8$] = 4 μM) with irradiation time. Data are expressed as mean values ± standard deviation of three separate experiments.

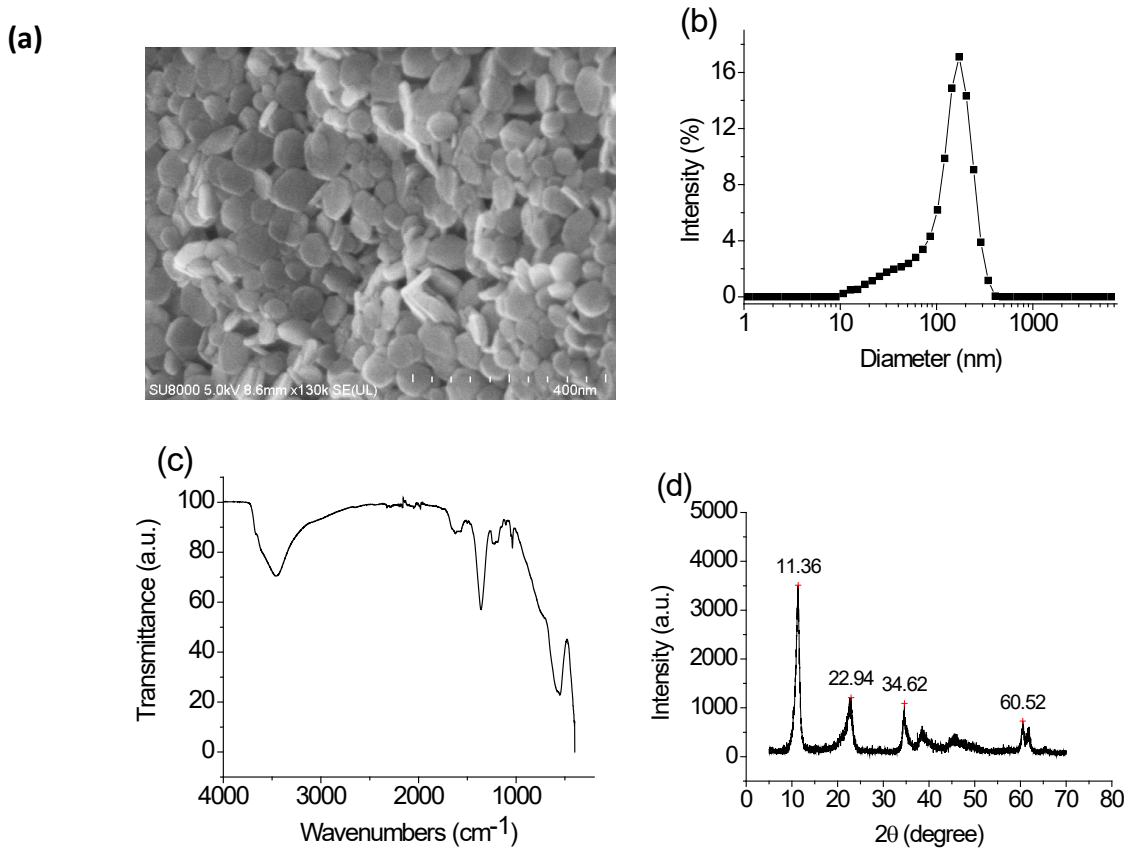

Figure S6. Characterization of LDH-S_2. (a) SEM image, (b) DLS measurement, (c) FTIR spectra, and (d) XRD patterns of LDH-S_2.

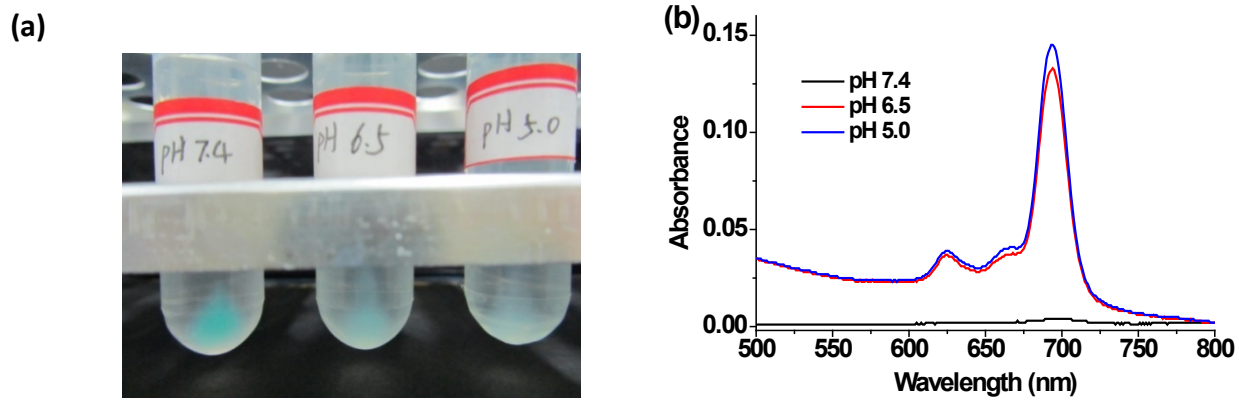

Figure S7. pH-controlled release of LDH-$ZnPcS_8$. (a) The photo of LDH-$ZnPcS_8$ suspension precipitated by centrifugation after incubation for 4 h in different pH solutions. (b) The corresponding UV-vis spectra of LDH-$ZnPcS_8$ in solution phase after 4 h incubation in different pH solutions.

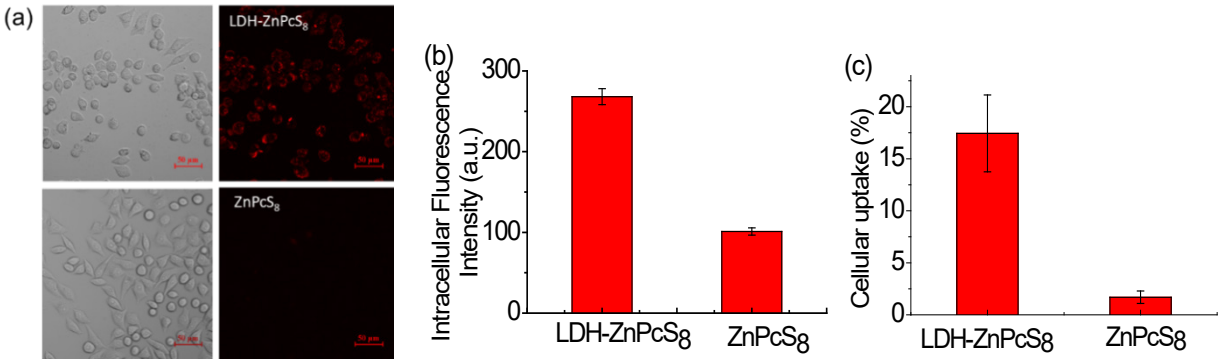

Figure S8. Cellular uptake of LDH-$ZnPcS_8$ and $ZnPcS_8$ by HepG2 cells. (a) The bright field (left column) and intracellular fluorescence (right column) images of HepG2 cells after incubation with LDH-$ZnPcS_8$ or $ZnPcS_8$ (both [$ZnPcS_8$] = 0.1 μM) for 2 h. Scale bars = 50 μm. (b) Comparison of the intracellular fluorescence intensities of LDH-$ZnPcS_8$ and $ZnPcS_8$. Data are expressed as the mean ± standard deviation (number of cells = 50). (c) Percentage of cellular uptake of LDH-$ZnPcS_8$ and $ZnPcS_8$ determined by an extraction method. Data are expressed as the mean ± standard error of the mean of three independent experiments.

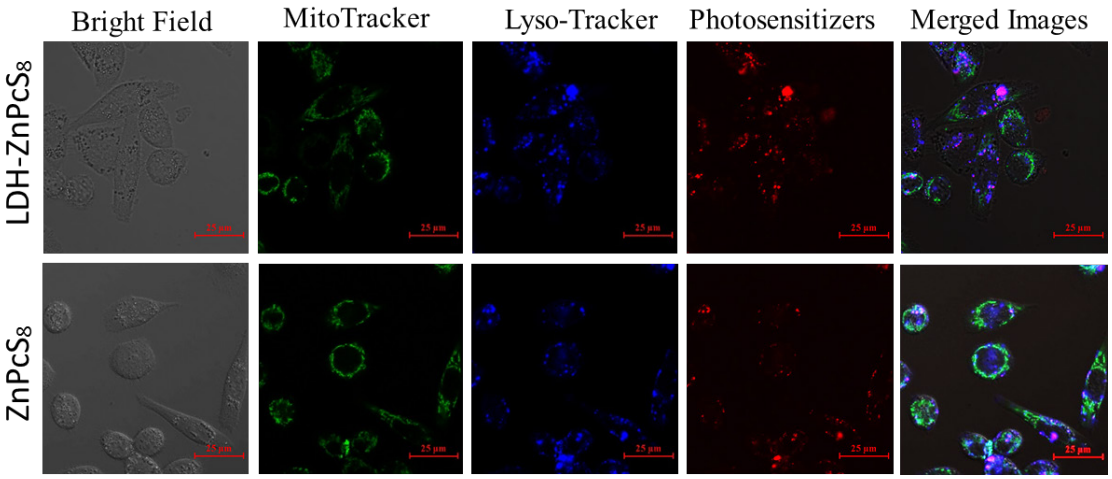

Figure S9. Subcellular localization of LDH-ZnPcS$_8$ and ZnPcS$_8$ in HepG2 cells. Visualization of the intracellular fluorescence of HepG2 cells by using filter sets specific for LDH-ZnPcS$_8$ and ZnPcS$_8$ (both [ZnPcS$_8$] = 0.1 μM) (in red, column 4), MitoTracker (in green, column 2), and Lyso-Tracker (in blue, column 3). The bright field images and the corresponding superimposed images are given in column 1 and column 5, respectively. Scale bars = 25 μm.

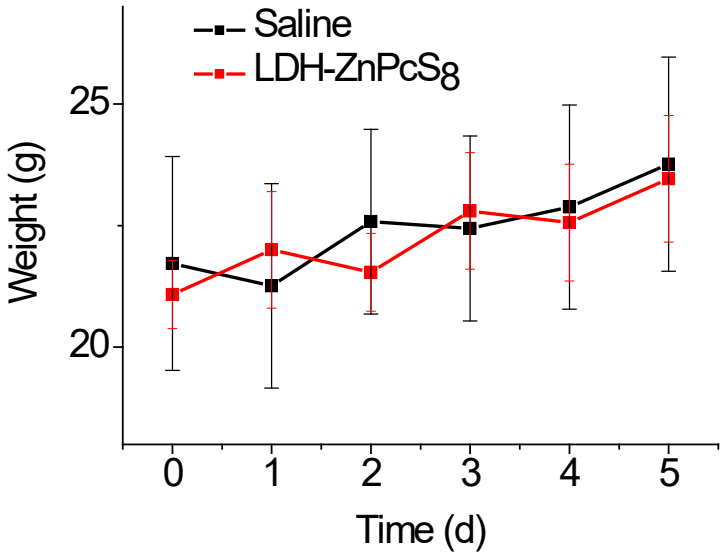

Figure S10. Body weight changing of mice after intravenous injection with saline or LDH-ZnPcS$_8$ and keeping them under room light.